# STATIC AND DYNAMIC BEHAVIOR OF OIL-LUBRICATED CYLINDRICAL AND ELLIPTICAL JOURNAL BEARINGS

**Marco Tulio C. Faria, mtcdf@uol.com.br**
Universidade Federal de Minas Gerais, Departamento de Engenharia Mecânica
Av. Antônio Carlos, 6627 – Belo Horizonte – MG – 31270-901

**Fernando de Assis G. Correia, fcorreia@zollern.com.br**
Zollern Transmissões Mecânicas Ltda
Av. Manoel Inácio Peixoto, 2147 - Cataguases – MG – 36771-000

***Abstract.*** *This work deals with the performance analysis of cylindrical and elliptical oil-lubricated journal bearings by using the finite element method. The Galerkin weighted residual method in conjunction with a linear perturbation method is applied on the classical Reynolds equation in order to render the zeroth- and first-order lubrication equations for the selected bearings. The thin fluid film domain is modeled through four-node rectangular isoparametric finite elements. The hydrodynamic pressure fields can be computed from the zeroth-order lubrication equations to allow the computation of the bearing static performance characteristics at several operating conditions. Furthermore, the first-order lubrication equations are solved to estimate the bearing dynamic force coefficients for different bearing geometric parameters. Static and dynamic performance characteristics of cylindrical and elliptical journal bearings are obtained in function of the Sommerfeld number and operating parameters. The results rendered in this work show that elliptical bearings present values of stiffness coefficients higher than those estimated for cylindrical bearings under low loading. Elliptical journal bearings offer more appropriate conditions for stable operation of rotating shafts than those provided by cylindrical journal bearings.*

***Keywords****: Cylindrical journal bearings, elliptical journal bearings, hydrodynamic lubrication theory*

## 1. INTRODUCTION

The hydrodynamic journal bearings are widely used in industrial turbomachinery due to their large capacity of carrying static and dynamic loads, to their stiffness and damping properties, and to their good capability of controlling the shaft center position (Sternlicht and Lewis, 1968; Knöss, 1980). The increasing demand for more efficiency and productivity in industrial processes has caused an increase in the rotating machinery operating speeds. Consequently dynamic problems associated with the oil-film instability have become very common in high speed industrial turbomachinery. Those problems have generally been addressed and minimized in the oil, petrochemical, chemical, and general process industries by two ways (Knöss, 1980; Vance, 1988): 1. raising the rotating shaft critical speeds by reducing the distance between the bearing supports; 2. replacing the journal bearings by a different type of bearing design. In operating industrial rotating machinery, the replacement of the bearing type becomes a more appealing solution to address the instability problems associated with the lubricant film because.

The fixed-geometry cylindrical journal bearings are the type of bearing widely used in industrial rotating machinery [Faria *et al*., 2006]. The cylindrical journal bearings not only consist on the cheapest design among all fixed-geometry bearings, but also possess low hydrodynamic stability, although have good capacity of carrying loads. On the other hand, variable-geometry bearings have been applied when the oil film stability is a crucial operating requirement, mainly in high speed turbomachinery. Variable-geometry bearings, such as the tilting pad journal bearings, present higher costs of manufacture, assembly, and maintenance than those related to fixed-geometry bearings (Allaire and Flack, 1981). Moreover, variable-geometry bearings require larger oil flow rates and present smaller stiffness and load capacity comparatively to the fixed-geometry bearings. Nowadays the search for fixed geometry bearing profiles that can meet the rigorous design requirements of industrial turbomachinery and the determination of the more appropriate design and operating parameters for oil film non-cylindrical journal bearings are still two big challenges for engineers, technicians, and designers of industrial rotating machinery.

In the technical literature, there is a large number of research works dealing with cylindrical journal bearings, but studies about other types of fixed-geometry bearing profiles are not common (Singh and Gupta, 1982). To exemplify this gap in the literature, only very recently the German Institute for Standardization (Deutsches Institut für Normung - DIN, 2007) has published notes about some non-cylindrical journal bearings.

In order to analyze the behavior of fixed geometry bearings, this paper presents the development of a finite element (FEM) procedure for oil-lubricated elliptical journal bearings. A linearized perturbation method (Lund, 1987) is applied on the classical Reynolds equation to render the zero-th- and first-order lubrication equations for elliptical bearings. The numerical solution of the lubrication equations permits to obtain the static and dynamic characteristics of elliptical journal bearings. The two main reasons for investing efforts in the study of elliptical journal bearings presented in this work are: *i*. the manufacturing costs of elliptical journal bearings are very similar to those of cylindrical journal bearings, well below to the costs of other fixed-geometry non-cylindrical journal bearing designs; *ii*. the surface wear

associated with start-up and cost-down operations, the bearing surface deformation related to sudden loading variations, and the induced strains generated during the bearing assembly change the cylindrical bearing profile along the time, transforming the cylindrical bearing into a non-cylindrical one. The results obtained in this work show several curves of steady-state and dynamic performance characteristics for elliptical journal bearings operating under stringent conditions. It is shown that elliptical journal bearings perform slightly better than cylindrical journal bearings from the point of view of oil-film stability.

## 2. GEOMETRY AND BASIC EQUATIONS FOR ELLIPTICAL JOURNAL BEARINGS

Figure 1 shows a schematic drawing of an elliptical journal bearing. The distance between the journal and bearing center centers is represented by the journal eccentricity *e*. *W* represents the applied load on the journal. The bearing length and diameter are described by *L* and *D*, respectively (*D*=2.*R*). The orthogonal axes (*X*, *Y*, *Z*) represent the inertial reference frame at the bearing center. The rotating system of coordinates (*x*, *y*, *z*) is attached to the journal Center (*x*=*R*.*θ*). The journal rotating speed is given by *Ω*. The bearing attitude angle is represented by □.

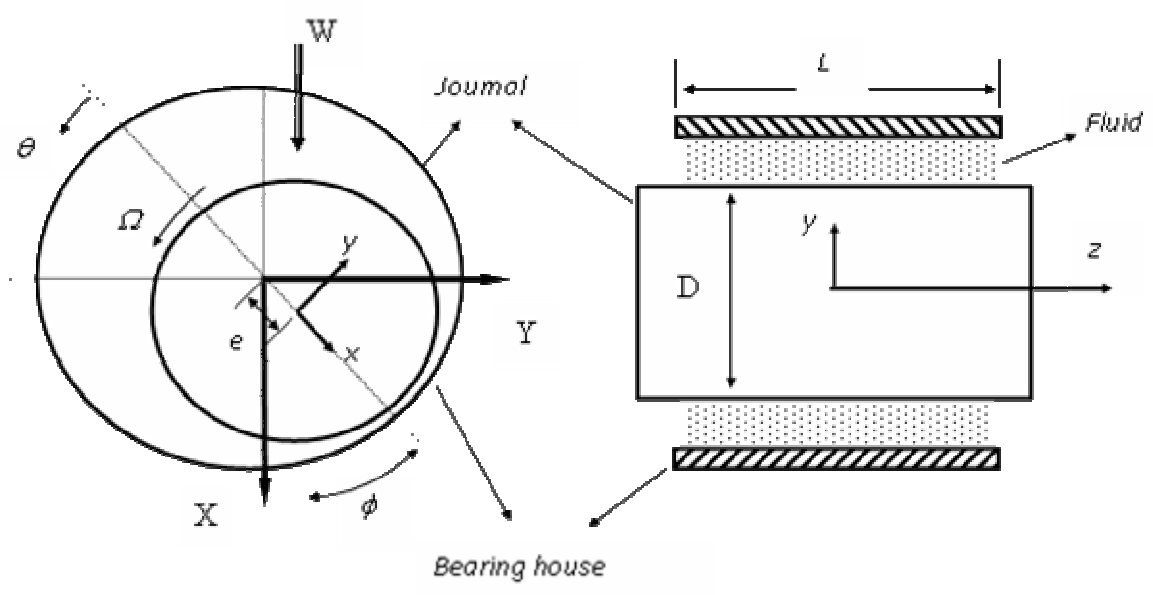


Figure 1. Schematic drawing of an elliptical journal bearing.

The classical Reynolds equation for an incompressible, istothermal, and isoviscous thin film flow can be expressed using cylindrical coordinates in the following form (Hamrock, 1994):

$$\frac{1}{R^2}\frac{\partial}{\partial\theta}\left(\frac{\rho h^3}{12\mu}\frac{\partial p}{\partial\theta}\right)+\frac{\partial}{\partial z}\left(\frac{\rho h^3}{12\mu}\frac{\partial p}{\partial z}\right)=\frac{1}{2}\frac{U}{R}\frac{\partial(\rho h)}{\partial\theta}+\frac{\partial(\rho h)}{\partial t} \tag{1}$$

where *R* is the journal radius, *p* is the hydrodynamic pressure, *h* the fluid film thickness, *U* represents the tangential speed of the journal shaft ($U = \omega R$), $\rho$ is the fluid mass density and $\mu$ is the fluid viscosity. The thin film fluid flow domain is described by $0 \le \theta \le 2\pi$ e $-L/2 \le z \le L/2$. The bearing hydrodynamic pressure is subjected to a periodic boundary condition along the circumferential direction, $p(\theta, z, t) = p(\theta + 2\pi, z, t)$. The bearing sides are at ambient pressure $p_a$, $p(\theta, L/2, t) = p(\theta, -L/2, t) = p_a$. The condition of half Sommerfeld is employed in the computation of the hydrodynamic pressure (Hamrock, 1994). The fluid film thickness "*h*" can be written in the following form.

$$h = c + e_x(t)\cos(\theta) + e_y(t)sen(\theta) + c.MP\|sen\theta\| \tag{2}$$

where the vertical and horizontal components of the journal eccentricity are expressed $e_x$ e $e_y$, respectively. The bearing radial clearance is given by *c*. *MP* represents the elliptical journal bearing preload (Correia, 2007).

## 3. DERIVATION OF THE LUBRICATION EQUATIONS

The computation of the bearing load capacity and dynamic force coefficients is performed using the lubrication equations obtained from the application of a linearized perturbation procedure on the Reynolds equation (Lund, 1987).

The journal equilibrium position ($e_{x_0}, e_{y_0}$) is perturbed by small amplitude motions at an excitation frequency $\omega$. Hence, the perturbed fluid thin film thickness can be written as.

$$h = h_0 + \left(\Delta e_x h_x + \Delta e_y h_y\right) e^{i\omega t} = h_0 + \Delta e_\sigma h_\sigma e^{i\omega t}; \qquad \sigma = x, y \tag{3}$$

where $h_0$ represents the steady-state or zero-th-order film thickness, $h_x = \cos(\theta)$, $h_y = \text{sen}(\theta)$ e $i = \sqrt{-1}$. Small oscillations in the fluid film thickness cause small perturbations in the hydrodynamic pressure field. The linearized perturbed hydrodynamic pressure field is expressed by.

$$p(\theta,t) = p_o(\theta,t) + (\Delta e_X p_X + \Delta e_Y p_Y) e^{i\omega t} = p_o + \Delta e_\sigma p_\sigma e^{i\omega t} \tag{4}$$

where $p_0$ represents the steady-state or zero-th-order hydrodynamic pressure, and $p_X$ e $p_Y$ are the first-order hydrodynamic pressures. Inserting Eqs. (3) and (4) into Eq. (1) renders the zero-th- and first-order lubrication equations for elliptical journal bearings, which are represented by Eq. (5) and Eq. (6), respectively.

$$\frac{1}{R^2}\frac{\partial}{\partial\theta}\left(\frac{\rho h_0^3}{12\mu}\frac{\partial p_0}{\partial\theta}\right) + \frac{\partial}{\partial z}\left(\frac{\rho h_0^3}{12\mu}\frac{\partial p_0}{\partial z}\right) = \frac{1}{2}\frac{U}{R}\frac{\partial(\rho h_0)}{\partial\theta} \tag{5}$$

$$\frac{1}{R^2}\frac{\partial}{\partial\theta}\left(\frac{3\rho h_0^2 h_\sigma}{12\mu}\frac{\partial p_0}{\partial\theta} + \frac{\rho h_0^3}{12\mu}\frac{\partial p_\sigma}{\partial\theta}\right) + \frac{\partial}{\partial z}\left(\frac{3\rho h_0^2 h_\sigma}{12\mu}\frac{\partial p_0}{\partial z} + \frac{\rho h_0^3}{12\mu}\frac{\partial p_\sigma}{\partial z}\right) = \frac{1}{2}\frac{U}{R}\frac{\partial(\rho h_\sigma)}{\partial\theta} + i\omega\rho h_\sigma \tag{6}$$

Bilinear shape functions $\Psi_i^e$ ($i$=1,2,3,4) (Bathe, 1982) are employed to represent the discrete zero-th- and first-order hydrodynamic pressure fields. Equation (5) represents the zero-th-order lubrication equation that allows the determination of the bearing pressure fields. The bearing dynamic force coefficients can be estimated from the first-order lubrication equation represented by Eq. (6). The zero-th- and first-order pressure fields are interpolated within a finite element domain $\Omega^e$ using the expressions $p_0^e = \Psi_i^e p_{0i}^e$ and $p_\sigma^e = \Psi_i^e p_{\sigma i}^e$, respectively, where $i$=1,2,3,4 and $\sigma$ = $X$,$Y$.

Within a finite element domain $\Omega^e$, the weighted-residual method of Galerkin is employed on Eq. (5) to render the discrete finite element zero-th-order lubrication equation, which is written as (Correia, 2007)

$$\left\{\iint_{\Omega^e}\frac{\rho h_0^3}{12\mu}\left(\frac{1}{R^2}\frac{\partial\Psi_i^e}{\partial\theta}\frac{\partial\Psi_j^e}{\partial\theta} + \frac{\partial\Psi_i^e}{\partial z}\frac{\partial\Psi_j^e}{\partial z}\right)d\Omega^e\right\}.p_{0i}^e = -\iint_{\Omega^e}\frac{\Omega}{2}\rho h_0\frac{\partial\Psi_j^e}{\partial\theta}d\Omega^e + \oint_{\Gamma^e}\Psi_j^e.\dot{m}_n d\Gamma^e \tag{7}$$

where $\dot{m}_n$ represents the lubricant mass flow through the finite element boundary $\Gamma^e$. Equation (7) consists of a linear system of algebraic equations that represent the steady-state form of the Reynolds equation within a finite element $\Omega^e$, which can expressed in the following form.

$$K_{ji}^e P_{0i}^e = f_j^e + q_j^e \tag{8}$$

The fluid matrix $K_{ji}^e$ can be obtained by using an integration scheme based on the Gauss quadrature (Bathe, 1982). The weighted-residual method of Galerkin is also used to render the finite element equations associated with the perturbed pressure Field, which are given as.

$$\begin{aligned}&\left\{\iint_{\Omega^e}\frac{\rho h_0^3}{12\mu}\left[\frac{1}{R^2}\frac{\partial\Psi_i^e}{\partial\theta}\frac{\partial\Psi_j^e}{\partial\theta} + \frac{\partial\psi_i^e}{\partial z}\frac{\partial\Psi_j^e}{\partial z}\right]d\Omega^e\right\}.P_{\sigma i}^e = \oint_{\Gamma^e}\Psi_j^e.\dot{m}_{1n}\,d\Gamma^e \\ &-\iint_{\Omega^e}\left\{\frac{3\rho h_0^2 h_\sigma}{12\mu}\left[\frac{1}{R^2}\frac{\partial p_0}{\partial\theta}\frac{\partial\Psi_j^e}{\partial\theta} + \frac{\partial p_0}{\partial z}\frac{\partial\Psi_j^e}{\partial z}\right] - \frac{\Omega}{2}\rho h_\sigma\frac{\partial\Psi_j^e}{\partial\theta} + i\varpi\rho h_\sigma\Psi_j^e\right\}d\Omega^e\end{aligned} \tag{9}$$

Equation (9) can be rewritten in matrix form as follows.

$$K^e_{\sigma ji}.p^e_{\sigma i} = q^e_{\sigma j} + f^e_{\sigma j} \tag{10}$$

The fluid film reaction forces can be estimated from Eq. (11), in which $p_a$ represents the ambient pressure.

$$F_{\sigma_o} = \int_0^L \int_0^{2\pi} (p_o - p_a) h_\sigma R.d\theta.dz \tag{11}$$

The computation of the first-order hydrodynamic pressure field is performed through a system of complex equations, which is obtained from the superposition of the finite element equations (Eq. (10)) over the fluid film flow domain. The numerical integration of the perturbed pressure field renders estimates for the complex impedance $\{Z_{\sigma\beta_o}\}_{\beta,\sigma=X,Y}$. The linearized bearing stiffness coefficients, $\{K_{\sigma\beta}\}_{\beta,\sigma=X,Y}$, and damping coefficients, $\{C_{\sigma\beta}\}_{\beta,\sigma=X,Y}$, associated with the hydrodynamic action of the perturbed fluid film, are expressed as.

$$Z_{\sigma\beta} = K_{\sigma\beta} + i\omega C_{\sigma\beta} = -\int_0^L \int_0^{2\pi} p_\beta h_\sigma R.d\theta.dz, \quad \beta,\sigma = X,Y \tag{12}$$

or

$$\begin{bmatrix} K_{XX} & K_{XY} \\ K_{YX} & K_{YY} \end{bmatrix} + i.\omega.\begin{bmatrix} C_{XX} & C_{XY} \\ C_{YX} & C_{YY} \end{bmatrix} = -\int_0^L \int_0^{2\pi} \begin{bmatrix} p_X h_X & p_Y h_X \\ p_X h_Y & p_Y h_Y \end{bmatrix} .R.d\theta.dz \cdot \tag{13}$$

## 4. RESULTS

Primarily, an example of elliptical journal bearing is selected to perform the mesh sensitivity analysis of the finite element procedure implemented in this work. The bearing baseline parameters are shown in Tab. 1. The predictions of bearing load capacity ($W$), direct stiffness coefficients ($K_{XX}$) and direct damping coefficients ($C_{XX}$) are obtained for different mesh sizes. Table 2 shows the results obtained in this example. The mesh size is represented by the global number of finite elements employed in the fluid film domain. A mesh with 2945 finite elements is chosen as a reference mesh in the computation of the relative errors. The results show that meshes with few elements can be used to render satisfactory results for the steady-stated and dynamic characteristics for the bearing analyzed.

Table 1. Elliptical bearing data for the mesh sensitivity analysis.

| | | |
|---|---|---|
| $c$ = 75.0 x $10^{-6}$ m | $MP$ = 0.30 | $D$ = 0.100 m |
| $\rho$ = 892.0 kg/m$^3$ | $L/D$ = 0.75 | $L$ = 0.075 m |
| $\mu$ = 8.4 x $10^{-3}$ | $\omega$ = 2000 rpm | $U$ = 10.47 m/s |

Table 2. Numerical results for the mesh sensitivity analysis.

| Number of finite elements | Load (N) | Relative error (%) | $K_{XX}$ (MN/m) | Relative error (%) | $C_{XX}$ (kN.s/m) | Relative error (%) |
|---|---|---|---|---|---|---|
| 340 | 1106.0 | 0.985 | 2.418 | 0.206 | 24230.0 | 1.062 |
| 600 | 1112.0 | 0.448 | 2.421 | 0.083 | 24370.0 | 0.490 |
| 810 | 1114.0 | 0.269 | 2.422 | 0.041 | 24410.0 | 0.237 |
| 1190 | 1116.0 | 0.090 | 2.423 | 0 | 24450.0 | 0.163 |
| 1480 | 1116.5 | 0.045 | 2.423 | 0 | 24470.0 | 0.082 |
| 1960 | 1117.0 | 0 | 2.423 | 0 | 24484.7 | 0.022 |
| 2330 | 1117,0 | 0 | 2.423 | 0 | 24490.0 | 0 |
| 2945 | 1117.0 | 0 | 2.423 | 0 | 24490.0 | 0 |

Secondly, an example of elliptical journal bearing (Singh and Gupta, 1982) is chosen to evaluate the accuracy of the finite element procedure developed. Predictions of the bearing load capacity rendered by the current finite element procedure (FEM) are compared with the results presented by Singh and Gupta (1982) for a bearing with slenderness ratio ($L/D$) equals to 1. Figure 2 depicts the curves of bearing dimensionless load capacity ($W^* = W/(p_a.L.D)$) versus the journal eccentricity ratio ($\varepsilon$=$e/c$) rendered by the FEM procedure comparatively to the results presented by Singh and Gupta. The finite element mesh in this example employs 1190 finite elements. The results for this example shows that there is a very good agreement between the FEM predictions and the values presented by Singh and Gupta for load capacity mainly at journal eccentricity ratios equal to or smaller than 0.5. For larger values of journal eccentricity ratio,

the maximum relative error does not reach 10%. This example of validation shows that the finite element procedure developed in this work can generate reliable predictions for elliptical journal bearing load capacity.

Now, the finite element procedure can be employed to analyze different oil-lubricated elliptical journal bearings. Two geometric parameters extremely important for the design of elliptical journal bearings are the preload (*MP*) and the slenderness ratio (*L*/*D*). If the preload is zero that means that the journal bearing has a circular profile. The analysis presented in this work aims at showing the influence of the bearing preload and slenderness ratio on the performance of elliptical journal bearings. The baseline parameters used for the bearing analysis are shown in Tab. 3. The finite element mesh uses 1190 bilinear finite elements in the modeling of the fluid film flow.

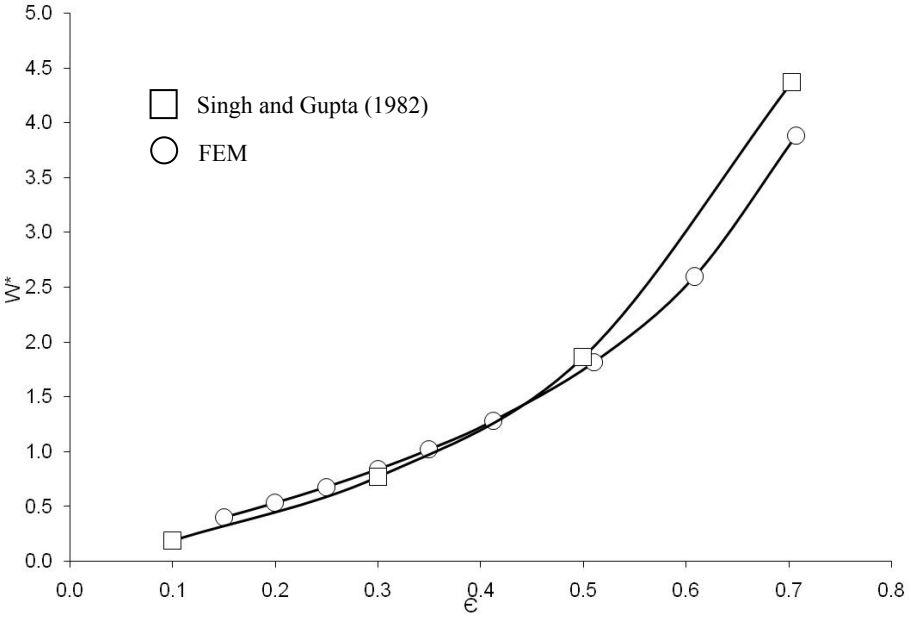


Figure 2. Curves of dimensionless load capacity versus eccentricity ratio for an elliptical journal bearing (*L*/*D* =1) obtained by Singh and Gupta (1982) and by the current finite element procedure (FEM).

Table 3. Baseline elliptical bearing parameters.

| | | |
|---|---|---|
| $D$ = 0.10 m | $MP$ = 0.1; 0.3; 0.5 e 0.7 | $c$ = 75.0x10$^{-6}$ m |
| $\omega$ = 2000 rpm | $L$ = 0.05 m; 0.075 m; 0.1 m | $\rho$ = 892.0 kg/m$^3$ |
| $\mu$ = 8.4 x 10$^{-3}$ Pa.s | $L/D$ = 0.5; 0.75 e 1.0 | $U$ = 10.47 m/s |

The Sommerfeld number ($S_o$) is a dimensionless number used to characterize journal bearings, including some bearing operating and geometric characteristics, and is expressed by $S_o = \frac{R^2}{c^2}.\mu.\frac{N}{P}$ (Shigley *et al*., 2003), where "*N*" represents the journal speed in hertz and "*P*" the bearing unit load ( $P = W / (L/D)$). Firstly, the curves of the Sommerfeld number versus eccentricity ratio are obtained for journal bearings with different values of preload (*MP* = 0.1; 0.3; 0.5 and 0.7) and slenderness ratio (*L*/*D*) of 1.0. Figure 3 depicts the influence of the preload and journal eccentricity on the bearing Sommerfeld number. The journal rotating speed of 2000 rpm is kept constant in this analysis. It can be noticed that the Sommerfeld number increases as the preload increases. Considering a journal bearings operating at constant speed, $S_o$ can be increased by using a lubricant with larger viscosity and or by reducing the journal eccentricity. The results presented in Fig. 3 indicate that non-cylindrical journal bearings are capable of supporting larger loads than cylindrical journal bearings do.

In order to show the influence of the slenderness ratio (*L*/*D*) on the static performance of elliptical bearings, at the same value of preload, Fig. 4 depicts four curves of the Sommerfeld number versus the journal eccentricity ratio for three values of (*L*/*D*). These curves show that the Sommerfeld number increases as the slenderness ratio decreases. Consequently, long bearings are able to support larger loads than short bearings do.

Another interesting analysis consists on predicting the bearing direct damping coefficients ($C_{XX}$ e $C_{YY}$) and the direct and cross-coupled stiffness coefficients ($K_{XY}$ e $K_{YX}$) for bearings under several operating conditions. The ratio of the direct damping coefficient to the cross-coupled stiffness coefficient permits to evaluate the level of effective damping provided by the fluid film bearing. Figure 5 depicts the curves of the bearing dimensionless damping coefficient ($C_{YY} = C.C_{YY}.\omega/W$) in function of the Sommerfeld number. The curves of the dimensionless cross-coupled stiffness coefficients ($K_{XY} = C.K_{XY}/W$) in relation to the Sommerfeld number are shown in Fig. 6. From the results presented in Fig.5 and

Fig.6, Pait can be noticed that the behavior of the direct damping coefficient is quite similar to that presented by the cross-couples stiffness coefficient.

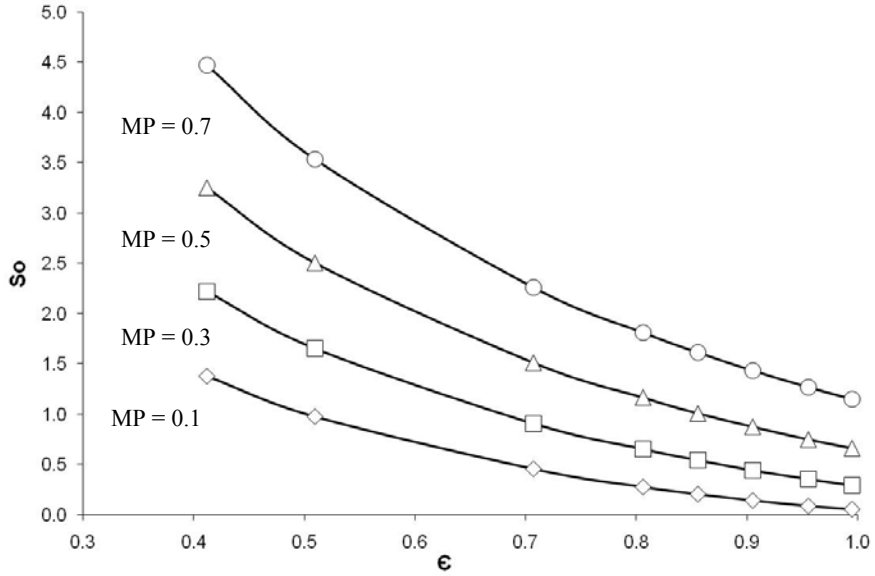


Figure 3. Curves of the Sommerfeld number versus the journal eccentricity ratio at four values of bearing preload ($L/D$ =1).

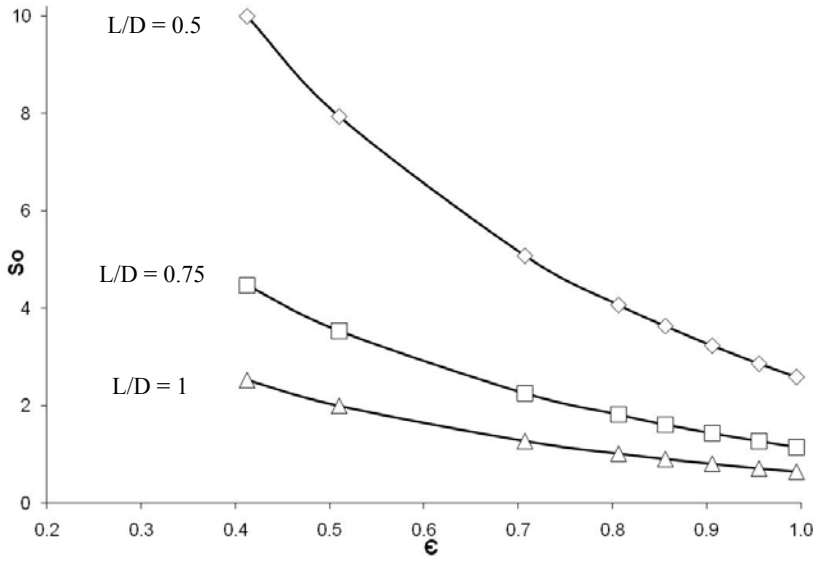


Figure 4. Curves of the Sommerfeld number versus the journal eccentricity ratio for bearings with different slenderness ratios.

Analyzing Fig.5 and Fig.6, it can be observed that for small values of the Sommerfeld number ($S_o$), close to zero, the values of the cross-coupled stiffness $K_{XY}$ are large and do not suffer influence of the ratio $L/D$. The analysis also shows that the cross-coupled stiffness coefficients $K_{XY}$ assumes small values for any value $L/D$ and $S_o$, in elliptical journal bearings. When the bearing presents large values of preload $MP$ and $S_o$, the cross-coupled stiffness $K_{XY}$ will exist only for small $L/D$. Then, it can be concluded that cylindrical journal bearings ($MP \approx 0$) are not adequate for conditions of low load (high $S_o$). Only elliptical journal bearings with high values of preload ($MP$) possess cross-coupled stiffness $K_{XY}$ (Correia, 2007).

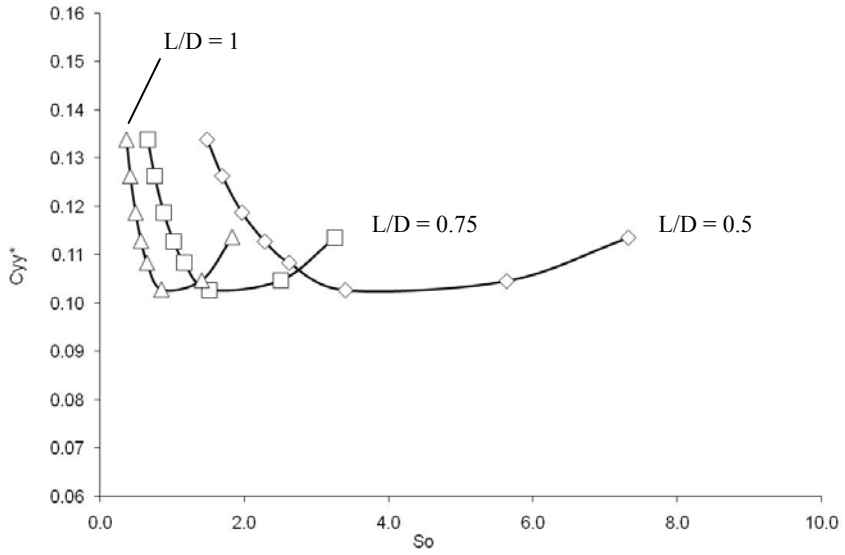


Figure 5. Curves of dimensionless direct horizontal damping coefficients $C_{YY}$ versus the Sommerfeld number at $MP$=0.5.

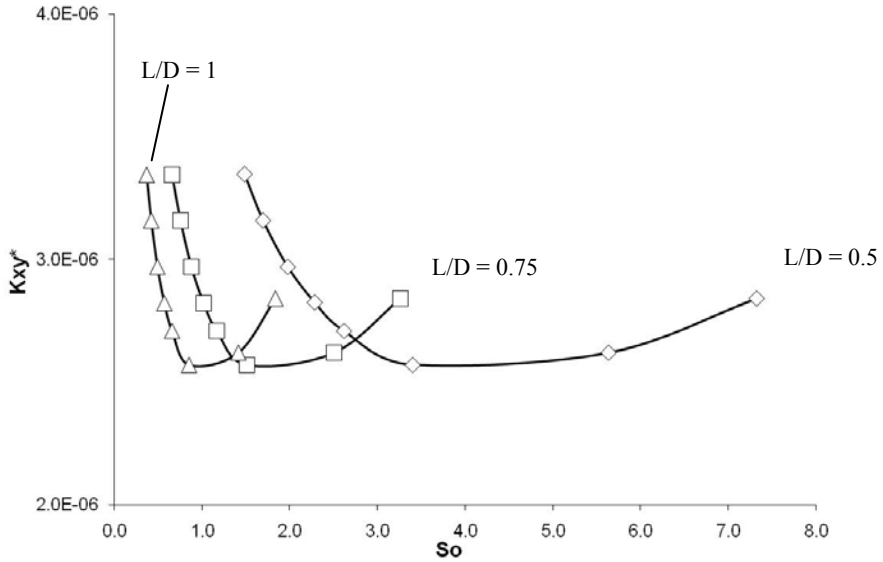


Figure 6. Curves of the dimensionless cross-coupled stiffness coefficients $K_{XY}$ versus the Sommerfeld number at $MP$=0.5.

## 5. CONCLUSIONS

This work presented a brief analysis of some steady-state and dynamic performance characteristics of elliptical journal bearings. The influence of some bearing geometric and operating parameters, such as the preload, the slenderness ratio, and the journal eccentricity, is analyzed by using a special finite element procedure. The numerical results rendered in this work show that cylindrical journal bearings can become unstable at high speeds and light loads. The elliptical journal bearings can be a good alternative for those operating conditions because they perform slightly better than cylindrical journal bearings. Several curves of bearing characteristics provide important subsides to understand the behavior of oil-lubricated elliptical journal bearings under different operating conditions and different geometric parameters. The results can help engineers and technicians to evaluate the applicability of elliptical journal bearings in a rotating machine. The analysis shows clearly that cylindrical journal bearings are not adequate for bearing applications with high values of the Sommerfeld number.

## 6. ACKNOWLEDGEMENTS

The financial support from FAPEMIG is gratefully acknowledged.

## 7. REFERENCES

Allaire, P.E. and Flack, R.D., 1981, "Design of Journal Bearings for Rotating Machinery", Proc. 10th Turbomachinery Symposium, Houston, USA, pp. 25-45.

Bathe, K.J., 1982, "Finite element procedures in engineering analysis". Ed. Prentice-Hall, Englewood Cliffs, NJ, USA, 734p.

Correia, F.A.G., 2007, "Determinação das características de desempenho de mancais radiais elípticos utilizando o método de elementos finitos", dissertação de mestrado em Engenharia Mecânica, Universidade Federal de Minas Gerais, Belo Horizonte, Brazil.

Faria, M.T.C., Correia, F.A.G. and Diniz, D.L.E., 2006, "Finite element procedure for analysis of oil-lubricated cylindrical journal bearings" (in Portuguese), Proc. XXVII Iberian Latin American Congress and Computational Methods in Engineering, Belém, Brazil, pp. 1-15.

DIN Institut fur Normung, 2007, "Gleitlager 2, Wekstoffe, Prufung, Berechnung, Begriffe Normen. Stand der abgedruckten Normen,. DIN-Taschenbuch, Herausgeber, Germany.

Hamrock, B.J., 1994, "Fundamentals of Fluid Film Lubrication", Ed. McGraw-Hill, New York, USA, 690p.

Knöss, K., 1980, "Journal bearings for industrial turbosets", Brown Boveri Review, Vol. 67, pp. 300-308.

Lund, J.W., 1987, "Review of the concept of dynamic coefficients for fluid film journal bearings", ASME Journal of Tribology, Vol. 109, pp. 37-41.

Shigley, J.E., Budynas, R.G. and Mischke, C.R., 2003, "Mechanical Engineering Design", McGraw-Hill, 7th Ed., New York, USA, 1059p.

Singh, A. and Gupta, B.K., 1982, "Stability limits of elliptical journal bearing supporting flexible rotors", Wear, Vol. 77, pp.159-170.

Sternlicht, B. and Lewis, P., 1968, "Vibration problems with high speed turbomachinery", ASME Journal of Engineering for Industry, Vol. 90, pp. 174-186.

Vance, J.M., 1988, "Rotordynamics of Turbomachinery", Ed. John Wiley & Sons, New York, USA, 388p.

## 8. NOMENCLATURE

| | |
|---|---|
| $c$ | Bearing radial clearance (m) |
| $C_{\alpha\beta}$ ( $\beta,\sigma = X,Y$ ) | Damping coefficients (N.s/m) |
| $D$ | Bearing diameter (m) |
| $e$ | Journal eccentricity (m) |
| $e_X$, $e_Y$ | Vertical and horizontal journal eccentricities (m) |
| $F_\sigma (\sigma = X,Y)$ | Bearing reaction forces (N) |
| $h$ | Fluid film thickness (m) |
| $h_0$ | Steady-state fluid film thickness (m) |
| $K_{\alpha\beta}$ ( $\beta,\sigma = X,Y$ ) | Stifness coefficients (N/m) |
| $L$ | Bearing length (m) |
| $MP$ | Bearing preload (m) |
| $p$ | Hydrodynamic pressure (Pa) |
| $p_a$ | Ambient pressure (Pa) |
| $p_0$ | Zero-order pressure (Pa) |
| $p_\sigma (\sigma = X,Y)$ | First-order pressure (Pa/m) |
| $P$ | Bearing unit load (N/m$^2$) |
| $R$ | Bearing radius (m) |
| $S_o$ | Sommerfeld number (dimensionless) |
| $U$ | Tangential velocity (m/s) |
| $W$ | Applied load (N) |
| $\varepsilon$ (=e/c) | Journal eccentricity ratio (dimensionless) |
| $\mu$ | Fluid viscosity (Pa.s) |
| $\rho$ | Fluid mass density (kg/m$^3$) |
| $\Psi_i^e$ | Shape functions |
| $\omega$ | Journal rotating speed (rad/s) |
| $\Omega^e$ | Finite element domain |

## 9. RESPONSIBILITY NOTICE

The authors are the only responsible for the printed material included in this paper.